

OPEN ACCESS

IOP Publishing

Superconductor Science and Technology

Supercond. Sci. Technol. **30** (2017) 015001 (6pp)

doi:10.1088/0953-2048/30/1/015001

Non-perturbative measurement of low-intensity charged particle beams

M Fernandes^{1,2,3}, R Geithner^{4,5}, J Golm⁴, R Neubert⁴, M Schwickert⁶,
T Stöhler^{4,5,6}, J Tan¹ and C P Welsch^{2,3}

¹CERN, CH-1211, Geneva 23 Switzerland

²Department of Physics, The University of Liverpool, Liverpool, L69 7ZE, UK

³Cockcroft Institute, Sci-Tech Daresbury, WA4 4AD, Daresbury, Warrington, UK

⁴Institute of Solid State Physics, Friedrich Schiller University, Jena, D-07737, Germany

⁵Helmholtz Institute Jena, Froebelstieg 3, D-07743 Jena, Germany

⁶GSI, Planckstrasse 1, D-64291, Darmstadt, Germany

E-mail: miguel.fernandes@cern.ch

Received 22 June 2016, revised 1 September 2016

Accepted for publication 30 September 2016

Published 2 November 2016



CrossMark

Abstract

Non-perturbative measurements of low-intensity charged particle beams are particularly challenging to beam diagnostics due to the low amplitude of the induced electromagnetic fields. In the low-energy antiproton decelerator (AD) and the future extra low energy antiproton rings at CERN, an absolute measurement of the beam intensity is essential to monitor the operation efficiency. Superconducting quantum interference device (SQUID) based cryogenic current comparators (CCC) have been used for measuring slow charged beams in the nA range, showing a very good current resolution. But these were unable to measure fast bunched beams, due to the slew-rate limitation of SQUID devices and presented a strong susceptibility to external perturbations. Here, we present a CCC system developed for the AD machine, which was optimised in terms of its current resolution, system stability, ability to cope with short bunched beams, and immunity to mechanical vibrations. This paper presents the monitor design and the first results from measurements with a low energy antiproton beam obtained in the AD in 2015. These are the first CCC beam current measurements ever performed in a synchrotron machine with both coasting and short bunched beams. It is shown that the system is able to stably measure the AD beam throughout the entire cycle, with a current resolution of 30 nA.

Keywords: accelerator diagnostics, low-intensity particle beams, cryogenic current comparator, SQUID


(Some figures may appear in colour only in the online journal)

1. Introduction

The non-perturbative detection and measurement of charged particle beams is an important aspect for different fields and applications relying on low-intensity beams. Low-intensity beams are found in areas as diverse as antimatter studies with antiprotons [1, 2], nuclear physics studies using rare isotope

beams [3, 4], hadron cancer therapy [5], mass spectroscopy [6] or ion implantation in semiconductor fabrication [7]. All these areas would profit from an online non-perturbing beam intensity measurement with absolute calibration.

Typical non-perturbative beam monitoring techniques rely on sensing the electromagnetic fields induced by the beam. Low-intensity beams present a considerable challenge due to the weak signals available to the diagnostic pickups, while, at the same time, the environment found in a particle accelerator usually generates high EMI background noise levels, which further complicate precise measurements. Traditional devices that are able to measure DC beams like the

 Original content from this work may be used under the terms of the [Creative Commons Attribution 3.0 licence](https://creativecommons.org/licenses/by/3.0/). Any further distribution of this work must maintain attribution to the author(s) and the title of the work, journal citation and DOI.

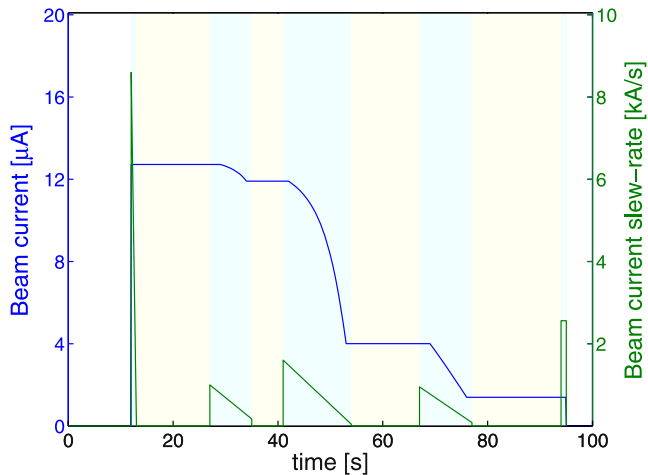


Figure 1. Evolution of the beam current and slew-rate along one AD cycle assuming a nominal injection and 100% efficiency. During the coasting beam phases the particle velocity is kept constant, and during the bunched phases particles are decelerated.

DC current transformer are limited in current resolution to $\sim 1 \mu\text{A}$ [8]. While Schottky-noise based monitors are very inaccurate when measuring low-intensity DC beams, and present a strong bunch length dependency for bunched beams [9], also these can not be easily calibrated for an absolute measurement.

2. Low-energy antiproton beams

The CERN low-energy antiproton (\bar{p}) physics experiments are currently served by the antiproton decelerator (AD) synchrotron. Its main purpose is to collect and decelerate the high-energy \bar{p} 's produced by colliding a proton beam against a fixed metal target [10, 11]. RF fields are used to decrease the beam energy, while beam cooling techniques are required to minimise the beam phase-space distribution and thus any particle losses. A precise measurement of the number of accumulated \bar{p} 's throughout the entire AD cycle is important to optimise the machine settings to deliver the maximum possible number of particles, and also to reduce the beam setup times. Currently, beam intensity measurement is provided by a Schottky-noise monitor that presents considerable limitations. During the debunched beam phases the accuracy and time resolution of the Schottky measurement is very poor, and during the bunched phases it is sensitive to the bunch longitudinal structure. Also, it does not allow for an absolute current calibration.

At the beginning of the AD deceleration cycle, shown in figure 1, \bar{p} 's are injected with a momentum of $3.57 \text{ GeV}/c$ corresponding to a velocity $\beta = 0.967$, and at extraction the momentum is $0.1 \text{ GeV}/c$ and $\beta = 0.106$. For a nominal injection, with $N = 5 \times 10^7 \bar{p}$, the beam electric current ranges from $12 \mu\text{A}$ to 300 nA . The AD cycle consists of different phases: during the beam cooling phases the beam is debunched and its velocity is kept constant, corresponding to the cycle flat-tops; during the deceleration phases the beam is

bunched and its velocity decreases, this corresponds to the cycle descending ramps; at beam injection and ejection beam is also bunched.

At injection the beam is composed of 4 bunches, each with a length of $4\sigma_t = 30 \text{ ns}$, assuming a Gaussian longitudinal shape. This is the moment when the current slew-rate reaches its highest value.

3. The cryogenic current comparator (CCC)

The CCC was first developed by Harvey in 1972 [12] for the precise measurement of DC current ratios in metrology systems, and a first proposal for utilising superconducting quantum interference device (SQUID) based diagnostics to measure beam current in a particle accelerator was made by Kuchnir at Fermilab [13]. Afterwards, the CCC was adapted and optimised for the measurement of particle beam currents by Peters *et al* at GSI [14] and Tanabe *et al* at INS [15]. Also, Vodel, Geithner *et al* [16–18] at DESY have used a CCC to measure electron dark currents from superconducting RF accelerating cavities. These projects used low-temperature superconductor technology and have shown the principle ability of CCC devices to measure beam currents with nA resolution. Other groups, including Hao *et al* [19] and Watanabe *et al* [20], have developed CCC devices using high-temperature superconductors but their current resolution was limited to values of the order of 100 nA .

Nonetheless, all these projects suffered from issues concerning sensitivity to mechanical vibrations and EMI perturbations. Furthermore, these setups were used for measuring slow beams, usually from transfer lines of accelerators, where the induced beam signal presented a reduced slew-rate, and were unable to measure short bunched beams presenting a high current slew-rate.

In collaboration between CERN, the GSI Helmholtz Centre for Heavy Ion Research, Friedrich Schiller University and Helmholtz Institute Jena, an operational CCC, adapted to the specific needs of the AD and extra low energy antiproton (ELENA) rings, has been successfully developed and tested. The functioning principle of the CCC is illustrated in figure 2. It is based on the measurement of the magnetic field induced by the particle beam to be measured [21]. The magnetic flux is concentrated in a high-permeability ferromagnetic pickup core from which it is coupled into the SQUID sensor via a superconducting flux transformer circuit. A superconducting magnetic shield structure containing the pickup core, with a meander structure [22], renders the coupled magnetic field nearly independent of the beam transverse position while also shielding the system against external magnetic field perturbations. A matching transformer is used to adapt the inductance of the pickup core L_p to the input inductance of the SQUID L_i , maximising the beam signal coupling to the SQUID.

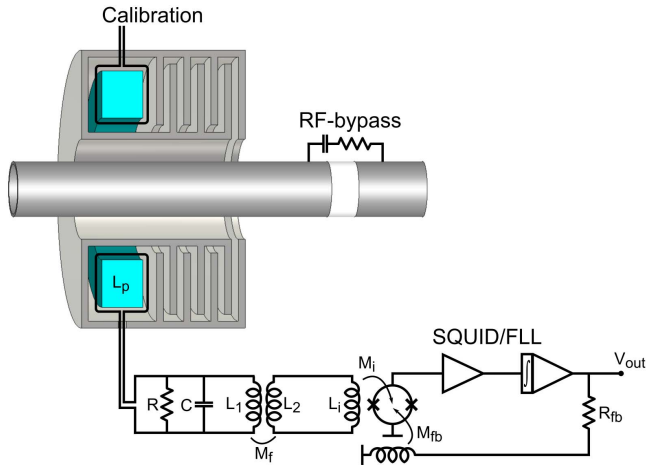


Figure 2. Schematic of the CCC, and the beam pipe with a ceramic gap. The cryostat structure consisting of a liquid helium tank, a radiation thermal shield and a vacuum vessel enclosing the monitor is not shown.

The coupling strength S_{I_B} is given by:

$$S_{I_B} = \frac{\phi_{\text{squid}}}{I_{\text{beam}}} = \left[\frac{M_i M_P M_f}{(L_P + L_1)(L_2 + L_i) - M_f^2} \right], \quad (1)$$

where M_P is the mutual inductance between the beam current and the pickup core coil self-inductance L_P , M_f is the mutual inductance of the matching transformer and $L_{1,2}$ are the respective primary and secondary self-inductances. The signal-to-noise ratio of the current measurement, when considering only the intrinsic noise sources, is enhanced by increasing the inductance factor of the pickup core. For a fixed geometry this is achieved by selecting ferromagnetic materials with high magnetic permeability at cryogenic temperatures as studied by Geithner *et al* in [23, 24]. SQUID devices are unparalleled in the sensitivity they exhibit to magnetic flux variations, but have a highly non-linear transfer function. Linearisation of the SQUID response is most commonly achieved with a readout scheme that implements a feedback loop with an integrator—the so called flux-locked loop (FLL) mode [25]. This scheme extends the dynamic range of SQUID systems, but also introduces a limitation on the maximum allowed slew-rate of the input signal, which is typically limited to less than 1–5 $M\phi_0/s$ (ϕ_0 is the magnetic flux quanta), depending on the level of coupled noise, bandwidth of feedback loop and length of cables. In order to keep the stability of the SQUID/FLL feedback loop, the slew-rate of the AD beam current signal needs to be strongly reduced.

4. AD implementation

The main design challenges were to adapt the CCC monitor to cope with the high slew-rate of the AD beam current while retaining its superior current resolution, to have a cryogenic system design so that the level of liquid helium in the monitor's cryostat is kept constant without the need for

periodic liquid-helium refills, with the cooling power provided by a cryocooler, and to optimise the mechanical performance by minimising the transmission of vibrations to the CCC. For the cryogenic system a new cryostat was designed and manufactured at CERN, and a commercial reliquifier unit with a pulse-tube cryocooler⁷ was used.

In the AD CCC the core has a single turn inductance $L_P = 104 \mu\text{H}$, while the SQUID device⁸ has an input coil self-inductance $L_i = 400 \text{ nH}$ and mutual inductance $M_i = 2 \phi_0/\mu\text{A}$. The obtained DC coupling strength is $S_{I_B} = 10.87 \phi_0/\mu\text{A}$. If this sensitivity was constant for all the frequency content of the injection signal, the slew-rate of the magnetic flux coupled to the SQUID at injection would be $93.5 \text{ G}\phi_0/s$. Considering the frequency dependency of the ferromagnetic pickup core permeability, made of Nanoperm [23], this value is reduced to $1.19 \text{ G}\phi_0/s$, which is still 3 orders of magnitude higher than the SQUID limit. Further reduction of the slew-rate was accomplished by inserting an RC-parallel filter in the primary coupling circuit, as shown in figure 2. Since the circuit loop needs to be kept superconducting in order to couple DC fields, it is not possible to add any series resistance. This imposes strong constraints on the exact configuration and order of the filter. The transfer function is given by:

$$S_{I_B}(s) = \frac{M_i'}{L_i' C} \times \left[\frac{1}{s^2 + s \frac{1}{RC} + \frac{1}{LC}} \right], \quad (2)$$

with $M_i' = \frac{M_i M_f}{L_i + L_2}$, $L_i' = L_1 - \frac{M_f^2}{L_i + L_2}$ and $\bar{L} = \frac{L_i' L_P}{L_i' + L_P}$.

The design bandwidth was set to 1 kHz, what allows for sufficient time resolution to probe into the beam physics effects of interest. This results in a reduction of the theoretical maximum slew-rate at the SQUID to $0.97 \text{ M}\phi_0/s$, which should be already under the SQUID/FLL limits. In order to increase the stability margin, an RF-bypass for the shielding beam mirror currents was installed in the ceramic gap of the beam pipe as shown in figure 2. Adding the RC filter in the SQUID coupling circuit presents the drawback that the thermal noise generated by R will be the dominant noise source, among the intrinsic noise sources (others are the SQUID/FLL electronics and the ferromagnetic core noise) [26], from 1 kHz down to the $1/f$ corner frequency, and equates to $\sim 300 \text{ pA Hz}^{-1/2}$. Still, this is low enough to permit a current resolution of the order of 10 nA.

The stability of the SQUID/FLL system to the AD beam injection current was confirmed by laboratory measurements using a stretched wire passing through the cryostat beam opening and a waveform generator. Figure 3 shows the measurement for successive injections of a bunched signal with an average current equal to $18 \mu\text{A}$, i.e. 50% more than the expected AD beam current at injection. The absence of a sustained strong drift indicates that the system is able to cope with the signal slew-rate, during the steady-state and during the even more demanding transient regime after each time the source was switched on and off, without significant flux-

⁷ Manufactured by Cryomech Inc.

⁸ Manufactured by Magnicon GmbH.

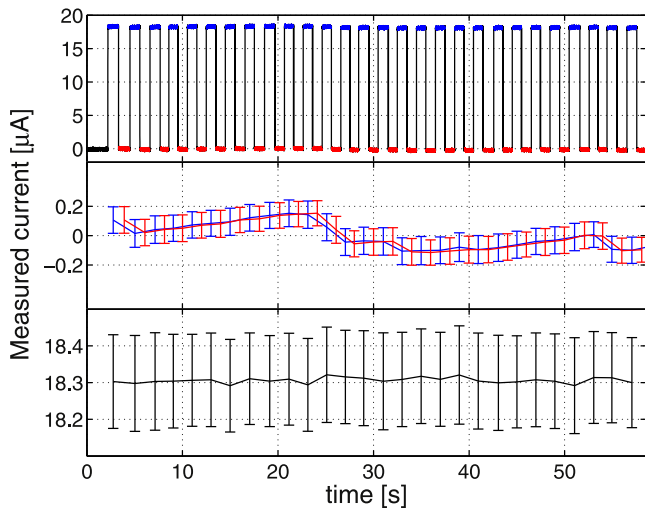


Figure 3. Laboratory measurement of a current signal with the same structure as found during the AD injection and plus 50% of average current which was repeatedly switched on and off. Top: measured current signal with top and bottom plateaus highlighted in blue and red, respectively; middle: absolute variation of the mean value of top and bottom plateaus referred to the average of the ensemble; bottom: absolute variation of difference between the mean values of top and bottom plateaus for successive transitions.

jumps. The long-term oscillations of the average current reading at the top and bottom values, observed in middle plot of figure 3, vary within ± 100 nA for the observed period and may have multiple origins. At low-frequencies (below ~ 500 Hz for Nanoperm [23]), the $1/f$ thermal noise due to the ferromagnetic core magnetic viscosity [26] becomes the dominant intrinsic noise source [27], which will cause long-term fluctuations. Also different external perturbations are known to affect the CCC reading, such as fluctuations in the pressure of the liquid helium bath in the cryostat or mechanical vibrations. Further studies still need to be conducted to identify and measure the different sources that may affect the measurement, and eventually implement methods to deconvolute and suppress these perturbations. It can also be observed that the noise level is of the order of 100 nA for both, zero and $18 \mu\text{A}$ average current plateaus.

5. AD beam measurements

The monitor was installed in the AD ring and measurements were taken during the 2015 physics run. Calibration of current measurement is performed by injecting a known current from a precision current source into the calibration loop shown in figure 2. Laboratory measurements comparing the response to a current injected into the calibration loop and into a beam simulating wire passing through the beam pipe section of the cryostat had shown compatible output values.

Measurements taken in the AD have shown an excess of noise at frequencies that are odd multiples of 50 Hz, which was the main cause for the degraded current resolution amounting to 275 nA. A significant flux jump was also observed in the SQUID/FLL working point, occurring at the

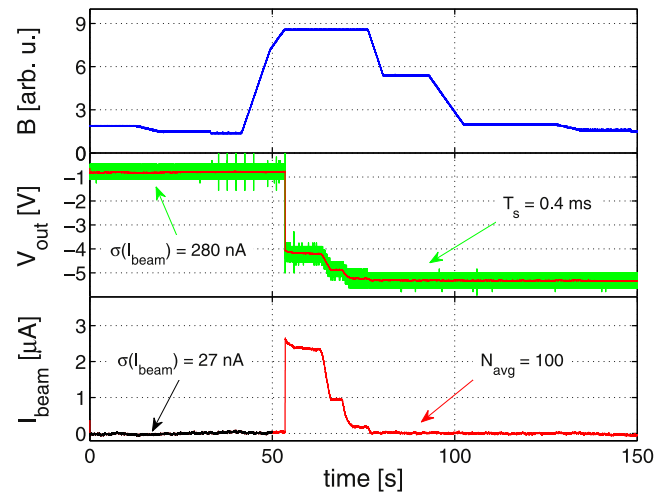


Figure 4. AD beam current measurement of one of the first cycles during beam setup. It is possible to observe the exact instants when beam was being lost. Top: AD dipole magnetic field cycle, which is proportional to the particle momentum. Beam is injected at beginning of top plateau and should be ejected at the end of second lowest plateau; middle: green trace is the raw CCC output signal; bottom: measured beam current obtained after applying a moving average filter, calibration and correction of offset at the moment of injection.

instant when two bunch rotation RF cavities are switched on (occurring once per cycle, around $50 \mu\text{s}$ after injection). Both these limitations can be seen in the middle plot of figure 4.

To address these two limitations the obtained raw signal was filtered using a time-domain moving average low-pass filter, and the baseline of the signal after the flux jump was recovered by summing an offset term, obtainable after the beam ejection when one knows that the beam current must be zero. This results in a measurement with current resolution of 30 nA, and a bandwidth of 11 Hz.

The measurement in figure 4 corresponds to a beam commissioning cycle where the beam was entirely lost during the first cooling plateau. The instants of beam loss are clearly visible, what represents a significant improvement over the existing Schottky measurement.

The number of circulating \bar{p} 's, to which we refer as the beam intensity, is obtained by normalising the measured current against the particle velocity according to equation (3), where L is the circumference of the AD-ring. In the AD cycle, $\beta_{\text{inj.}} = 0.97$ at injection plateau and $\beta_{\text{ej.}} = 0.11$ at ejection.

$$N = \frac{L}{ec} \times \frac{I}{\beta}. \quad (3)$$

Figure 5 shows the intensity measurement for one AD cycle derived from the CCC current measurement using equation (3). The sampling rate on the beam current signal was 1 kHz, after applying the moving average filter with $N = 100$ the bandwidth was reduced to 4.4 Hz. In this measurement one can observe that $(3.555 \pm 0.008) \times 10^7 \bar{p}$ are first injected in the ring, and $(2.50 \pm 0.05) \times 10^7 \bar{p}$ remain at the moment of ejection. This represents a loss of 30% for this particular cycle. The improvement obtained with the CCC

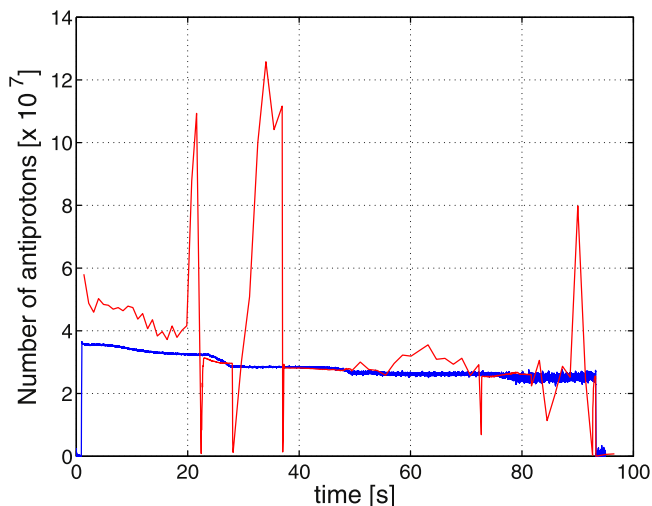


Figure 5. Derived number of antiprotons circulating in the AD ring for an entire cycle. The plot shows the comparison between the measurement obtained with the existing Schottky monitor (in red) and the CCC (in blue).

measurement over the Schottky one is clearly visible, particularly during the beam cooling phases, where the Schottky measurement presents a very bad resolution and accuracy due to the poor signal-to-noise ratio of the coasting beam signals. The CCC intensity measurement, on the other hand, is independent of the beam state along the AD cycle, i.e. whether it is bunched or not, achieving the same performance independently of the beam time structure. However, the absolute error of the intensity measurement increases with decreasing particle velocity, what is visible in figure 5.

6. Conclusions and outlook

A CCC monitor optimised for the AD and ELENA rings at CERN has been implemented and first measurements with beam have been carried out. These are the first CCC beam current measurements performed in a synchrotron using both coasting and short bunched beams.

The CCC is currently the only device able to measure non-perturbatively low intensity DC beams. A particular improvement is the possibility of absolute calibration of the experiments receiving the particle beam using data from the CCC, as well as cross-calibration of other intensity monitors for which no simple calibration method is available. A current intensity resolution of 30 nA was successfully demonstrated after low-pass filtering with a cut-off frequency at 10 Hz. The system was able to cope with a beam current signal slew-rate exceeding 8 kA s^{-1} maintaining the SQUID/FLL stability. The new cryostat mechanical design provided for an excellent decoupling of mechanical perturbations, enabling the CCC monitor to attain this performance even when the connected cryocooler unit was operating.

The excess of noise observed, primarily at 50 Hz and higher harmonics, is suspected to be due to stray currents flowing in the beam pipe that are then picked up by the

monitor. Also the flux-jump occurring at the moment of injection is suspected to be generated by high-frequency stray currents circulating in the beam pipe at the moment of the discharge of bunch rotations cavities. The RF-bypass, installed in the ceramic gap shown in figure 2 in order to reduce the beam signal slew-rate, may be responsible for these two limitations. As part of future optimisation studies it will be considered the modification and relocation of this bypass.

Acknowledgments

The authors acknowledge the outstanding work of CERN's Central Workshop (EN-MME) and Cryogenic group (TE-CRG) in designing, fabricating and testing the cryostat. Fruitful discussions with Patrick Odier, Jeroen Belleman, Manfred Wendt, Henry-Jobes Barthelmess and Dietmar Drung are gratefully acknowledged.

This project has received funding from the European Unions Seventh Framework Programme for research, technological development and demonstration under grant agreement number 289485. Open access funding provided by the University of Liverpool.

References

- [1] Amoretti M *et al* 2002 Production and detection of cold antihydrogen atoms *Nature* **419** 456–9
- [2] Hori M and Walz J 2013 Physics at CERN's antiproton decelerator *Prog. Part. Nucl. Phys.* **72** 206–53
- [3] Eschke J 2005 International facility for antiproton and ion research (FAIR) at GSI, darmstadt *J. Phys. G: Nucl. Part. Phys.* **31** S967
- [4] Welsch C P and Ullrich J 2006 Flair—a facility for low-energy antiproton and ion research *Hyperfine Interact.* **172** 71–80
- [5] Linz Ü (ed) 2012 *Ion Beam Therapy Fundamentals, Technology, Clinical Applications* 1st edn (Berlin: Springer)
- [6] Calvo E C, Santos F J, López-Gutiérrez J M, Padilla S, García-León M, Heinemeier J, Schnabel C and Scognamiglio G 2015 Status report of the 1 MV AMS facility at the centro nacional de aceleradores *Nucl. Instrum. Methods Phys. Res. B* **361** 13–9, *The 13th Accelerator Mass Spectrometry Conf.*
- [7] Ziegler J F 1988 *Ion Implantation Science and Technology* 2nd edn (New York: Academic)
- [8] Odier P, Ludwig M and Thoulet S 2009 The dcct for the lhc beam intensity measurement *Technical Report CERN-BE-2009-019* CERN, Geneva
- [9] Peterson D W 1991 Schottky signal monitoring at fermilab *AIP Conf. Proc.* **229** 108–30
- [10] Belochitskii P, Eriksson T and Maury S 2004 The CERN antiproton decelerator (AD) in 2002: status, progress and machine development results *Nucl. Instrum. Methods Phys. Res. B* **214** 176–80, *Low Energy Antiproton Physics (LEAP'03)*
- [11] Maury S 1997 The antiproton decelerator: Ad *Hyperfine Interact.* **109** 43–52
- [12] Harvey I K 1972 A precise low temperature dc ratio transformer *Rev. Sci. Instrum.* **43** 1626–9
- [13] Kuchnir M, McCarthy J and Rapidis P 1985 SQUID based beam current meter *IEEE Trans. Magn.* **21** 997–9

- [14] Peters A, Vodel W, Koch H, Neubert R, Reeg H and Schroeder C H 1998 A cryogenic current comparator for the absolute measurement of Na beams *AIP Conf. Proc.* **451** 163–80
- [15] Tanabe T, Chida K and Shinada K 1999 A cryogenic current-measuring device with nano-ampere resolution at the storage ring TARN II *Nucl. Instrum. Methods Phys. Res. A* **427** 455–64
- [16] Geithner R, Neubert R, Vodel W, Seidel P, Knaack K, Vilcins S, Wittenburg K, Kugeler O and Knobloch J 2011 Dark current measurements on a superconducting cavity using a cryogenic current comparator *Rev. Sci. Instrum.* **82** 013302
- [17] Vodel W, Neubert R, Nietzsche S, Knaack K, Wendt M, Wittenburg K and Peters A 2003 Cryogenic current comparator for absolute measurements of the dark current of superconducting cavities for tesla *IEEE Trans. Appl. Supercond.* **13** 743–6
- [18] Vodel W, Neubert R, Nietzsche S, Seidel P, Knaack K, Wittenburg K and Peters A 2007 A new measurement tool for characterization of superconducting rf accelerator cavities using high-performance Its squids *Supercond. Sci. Technol.* **20** S393
- [19] Hao L, Macfarlane J C, Peden D A, Lee R A M, Gallop J C and Carr C 2001 Design and performance of an HTS current comparator for charged-particle-beam measurements *IEEE Trans. Appl. Supercond.* **11** 635–8
- [20] Watanabe T, Watanabe S, Ikeda T, Kase M, Sasaki Y, Kawaguchi T and Katayama T 2004 A prototype of a highly sensitive cryogenic current comparator with a HTS SQUID and HTS magnetic shield *Supercond. Sci. Technol.* **17** S450–5
- [21] Geithner R, Kurian F, Reeg H, Schwickert M, Neubert R, Seidel P and Stöhlker T 2015 A squid-based beam current monitor for FAIR/CRYRING *Phys. Scr.* **T166** 014057
- [22] Grohmann K, Hahlbohm H D, Hechtfisher D and Lübbig H 1976 Field attenuation as the underlying principle of cryo current comparators *Cryogenics* **16** 423–9
- [23] Geithner R, Heinert D, Neubert R, Vodel W and Seidel P 2013 Low temperature permeability and current noise of ferromagnetic pickup coils *Cryogenics* **54** 16–9
- [24] Steppke A, Geithner R, Hechler S, Nawrodt R, Neubert R, Vodel W, Schwickert M, Reeg H and Seidel P 2009 Application of Its-squids in nuclear measurement techniques *IEEE Trans. Appl. Supercond.* **19** 768–71
- [25] Drung D and Mück M 2004 *The SQUID Handbook* vol I ed J Clarke and A I Braginski (Weinheim: Wiley-VCH) pp 127–70
- [26] Durin G, Falferi P, Cerdonio M, Prodi G a and Vitale S 1993 Low temperature properties of soft magnetic materials: Magnetic viscosity and 1/f thermal noise *J. Appl. Phys.* **73** 5363
- [27] Sese J, Camon A, Rillo C and Rietveld G 1999 Ultimate current resolution of a cryogenic current comparator *IEEE Trans. Instrum. Meas.* **48** 1306–13